AIRCRAFT LOADS – A WIDE RANGE OF DISCIPLINARY AND PROCESS-RELATED ISSUES IN SIMULATION AND EXPERIMENT

T. Klimmek[1], R. Bogenfeld[2], E. Breitbarth[3], J. Dillinger[1], V. Handojo[1], T. Kier[4],
D. Kohlgrüber[5], M. Pusch[4], C. Raab[6], and J. Wild[7]

DLR, German Aerospace Center,

[1]Institute of Aeroelasticity, Göttingen, [2]Institute of Composite Structures and Adaptive Systems, Braunschweig, [3]Institute of Materials Research, Köln, [4]Institute of System Dynamics and Control, Oberpfaffenhofen, [5]Institute of Structures and Design, Stuttgart, [6]Institute of Flight Systems, Braunschweig, [7]Institute of Aerodynamics and Flow Technology, Braunschweig

Summary

The estimation of the loads is a key aspect of the extensive aircraft design process and also an important task during the life-time of an aircraft. DLR's joint efforts regarding the loads estimation and application, the latter also in view of structural aspects, both simulation based and experimentally were part of the DLR project KonTeKst (2016-2019). The loads activities cover the loads process, with one focus on the component loads process. Therein, the various possibilities to introduce loads to the structure were investigated as well as the consideration of flight control methods. On the structural side experiments were executed to estimate damage tolerance parameters for composite structures. Furthermore, fatigue and damage tolerance properties of metallic fuselage structures were estimated. Therefore, a novel AlCuLi sheet material was investigated regarding anisotropic fatigue crack growth. Finally, the consideration of aerodynamic loads for high lift configurations was investigated. The experimental investigations comprise flight tests to measure loads as well as a special wind tunnel test to investigate loads control. For the DLR research glider Discus-2c, the wing loads measured with calibrated electrical strain gauge were compared to the loads determined from the pressure sensors (MEMS), distributed around a wing section. For the DLR HALO, a Gulfstream G550, the loads at special measurement devices attached to the wing used for atmospheric investigation, were measured. Eventually, the structural design of a wind tunnel model with movable control surfaces was done as well as the execution of wind tunnel tests in the DLR's Crosswind Test Facility (SWG), the latter by applying active loads control even in failure cases.

Keywords: aircraft loads, loads process, component loads, loads control, fatigue, damage tolerance, material properties, composite material, loads flight testing, structural design, wind tunnel testing

1. INTRODUCTION

Loads accompany the life of an aircraft from the first sketch up to its very end, in a way from "the cradle to the grave". Therefore, the discipline aircraft loads is not only required during the design of a new aircraft. The predicted and the unpredicted loads an aircraft endures during lifetime have to be taken into account for its maintenance and to assess its structural integrity.

In [1] the comprehensive topic "aircraft loads" is outlined for military aircraft. Therein also the aspect of converting overall aircraft loads (external loads) into component loads is shown in principal. Besides the estimation of aircraft loads by applying proper simulation methods and using applicable simulation models in the design phase, the appraisal of loads by utilizing experiments, also during lifetime, is eminent as well. Such experiments range from wind tunnel tests, via various structural tests, up to flight tests.

DLR took care of the topic "aircraft loads" for the first time in a comprehensive way in the project iLOADS (2012-2015) [2]. Therein DLR's specific needs, requirements, and tasks with respect to the subject aircraft loads were put together as well as DLR's individual loads process(es). The latter also due to the fact that DLR is not an aircraft manufacturer, but operates a fleet of aircraft ranging from sailplanes (Discus-2c) via business jets modified for research purposes (e.g. Gulfstream G550 HALO), up to a transport aircraft for 150PAX (Airbus A320-200 ATRA). As so-called "Entwicklungsbetrieb" DLR is also allowed to execute specific tasks in the frame of the certification of an aircraft, like supplemental type certificate (STC) tasks. An STC is a type certificate (TC) issued when an applicant like DLR has received approval from the corresponding authority to modify an aircraft from its original design.

Within the DLR project KonTeKst (2016-2019) [3] the comprehensive activities with respect to aircraft loads were continued, with regard to the development and operation of short range aircraft, the main topic of KonTeKst. Regarding the loads topic basically four tasks were pursued. At first the documentation of the status of DLR's specific loads process(es) with respect to the needs, the load cases, the tools, and the processes was continued (chapter 2). A special focus was also put on the component loads process, by investigations on the loads analysis with and without control and the loads application as well as on basic and practical structural and material aspects and loads relevant aerodynamics for high lift configurations (chapter 3). The loads measurement during flight testing was another focal point of the project (chapter 4). Finally, the design, manufacturing and testing of a wind tunnel model of a wing, where active loads control methods were developed and successfully applied, was a final high-light of the project (chapter 5)

2. LOADS PROCESS – DEFINITION AND DOCUMENTATION

Based on the results of the DLR project iLOADS [2], [4] in KonTekst the field of „loads analysis within DLR" was further developed. A special emphasis was put on the component loads process.

Assessment of Needs

Already within iLOADS a needs assessment has been established. The field of loads analysis was structured by bringing together the various topics of the loads analysis, and also aspects and subject areas closely connected to the loads process. Therein also the corresponding DLR institutes were assigned on. In FIGURE 1 the core loads process and the adjacent fields are shown.
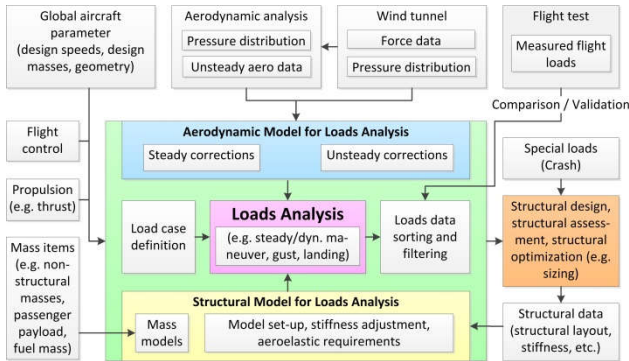

FIGURE 1 Core load process and corresponding topics

Besides the further development of the DLR loads process the field of "virtual certification" in the frame of the "digitalization in aeronautics" was detected as new topic. First efforts have been undertaken within the DLR project ViCert. Therein the aspect of provenance of the data processed and created in the frame of a loads process were investigated

Load Cases

For the systematic categorization of the load cases the concept developed in the DLR project iLOADS has been further developed and applied within KonTeKst. Furthermore in the DLR project VicToria the defined conventions were applied. The concepts results for example in naming rules for data files. Thereby the data files for the mass models are straightforward applicable, e.g. to set up or respectively combine different mass models for specific mass configurations according to the requirements of the individual load cases (mass model empty weight + mass model fuel + mass model payload). The naming conventions are furthermore used for the reporting of the load case or mass case.

Tools

The loads process consists of a number of computer programs, the so-called „tools". They execute different tasks in the frame of the loads analysis. The tools can be referred to the basic steps of the loads process: load case definition, loads analysis, and loads post processing.

In addition to the loads analysis tools MSC Nastran and VarLoads, both were already mentioned and are still most of all used for loads estimation, the new loads analysis tool LoadsKernel has been developed at DLR-AE over the last years. Like VarLoads, the LoadsKernel uses stiffness and mass matrices (e.g. from MSC Nastran) as input for comprehensive loads analyses. The LoadsKernel was primarily applied within the DLR projects Mephisto and Diabolo. Though, for the project KonTeKst the LoadsKernel was be used to simulate several periods of time from the flight test campaign of the Discus-2C. Therewith global flight parameters, like the angle of attack, could be verified.

Processes

With the focus on the process aspect of the loads process several requirements are to be defined. The defined loads process can be fully automatized, partly, or completely manual. The parts of the loads process have to be defined as well as the interfaces. In aircraft design tasks the loads process part of a design process, where the loads are used for the structural design. The principal parts of a loads process as part of a design process are shown in FIGURE 2.

The fully automatized aeroelastic design process cpacs-MONA [5] is such a design process with an integrated loads process. Input and output data format is CPACS, an xml data format defined by DLR [6].

The loads analysis for certification, e.g. to be used for certification task of aircraft of the DLR fleet, can be limited to the kernel loads process. Therefore the design loads or critical loads have to be estimated and properly documented. Such documentation has to be in line with requirements given by the regulations of the corresponding authorities.

With respect to the mentioned topic of provenance, the aeroelastic design process cpacs-MONA has been scrutinized within the DLR project ViCert.
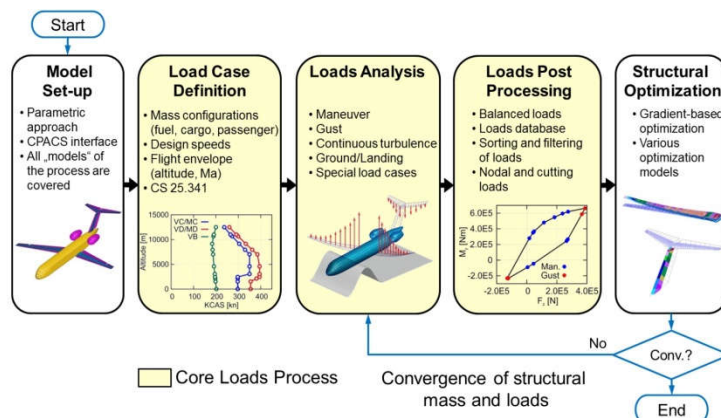

FIGURE 2 Basic loads Process as part of a parametric design process like cpacs-MONA

3. COMPONENT LOADS PROCESS

3.1 Component Loads Analyses

Structural modeling of control surfaces

For the project KonTeKst, the FE model of the D150 – which is the reference aircraft in the project – is extended by structural models of the primary control surfaces (ailerons, elevators, rudder). These are connected to the main structure with massless bars and hinge springs as visualized in FIGURE 3 This extension enables a more detailed loads analysis of the control surfaces.
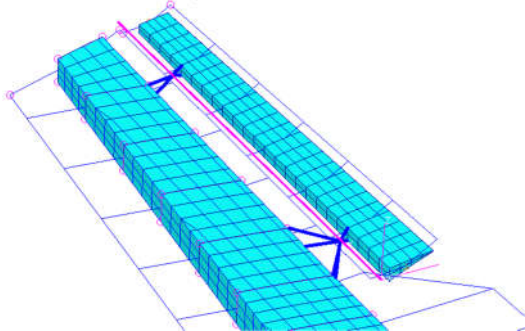

FIGURE 3 FE model of an aileron an attachment

Splining of aerodynamic forces

On the aerodynamic side, splining variants for the aerodynamic forces are investigated, see FIGURE 4. The default spline is variant 1 where the aerodynamic forces are splined onto the grids on the leading edge, trailing edge and the reference axis. With a finer distribution of the aerodynamics forces as in variant 2, the differences in the cutting loads are below 2%, and the variations in the von-Mises stresses are below 1%.
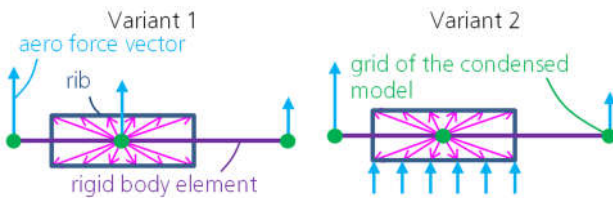

FIGURE 4 Variants of aerodynamic force spline

Load spectra of selected shell elements

For selected elements on the wing lower skin, the load spectra due to continuous turbulence are calculated using the transfer functions of the major principal stresses as a response to vertical wind. In doing so, the von-Kármán turbulence spectrum is taken into account, and the probability distribution of the turbulence intensity is based on MIL-STD-1797A [7]. With this load spectrum analysis, a more individualized fatigue analysis for the concerning aircraft can be carried out.

3.2 Loads Analysis with Controls

The employment of Flight Control Laws (FCL) augments the flight characteristics of an airplane to meet criteria related to handling qualities and other flight mechanical design specifications. These control laws can fundamentally change the dynamics of the aircraft, which in turn has a considerable effect on the structural loads. Therefore, in the loads analysis the closed loop aircraft needs to be considered when simulating gust and turbulence encounters as well as transient design manoeuvres [8].

However, typically loads models neglect important aspects of flight dynamics, which are essential for the design of the primary flight control laws, as e.g., the roll-yaw coupling is relevant for the flight mechanical eigenmodes like the dutch roll mode or the induced drag has a major influence on the phugoid motion. All these effects are unaccounted for in the Doublet Lattice Method (DLM), since in-plane forces are neglected.

To circumvent the problem associated with the neglected force contributions, the 3D-Panel Method NEWPAN [9] is employed. FIGURE 5 depicts the computational grid for the panel method and the DLM.
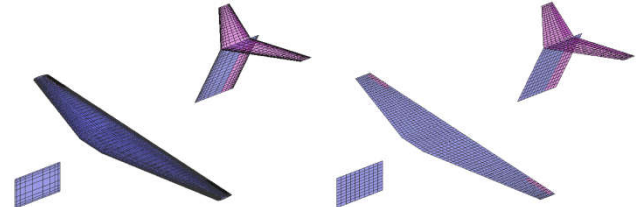

FIGURE 5 Computational grids for the 3D-Panel Method (left) and the Doublet Lattice Method (right)

Similarly to the DLM, the panel method provides Aerodynamic Influence Coefficient matrices (AICs) linearized about a given flight state. Also, frequency dependent unsteady AICs can be used in the usual way for frequency domain gust analysis or, after appropriate transformation, in a time simulation [10]. FIGURE 6 shows the lift and in-plane forces over the wing span for the DLM and the 3D panel method. As expected, the DLM fails to account for the force in the x-direction. Also, note the changes in lift and hence rolling moment due to the yawing motion.
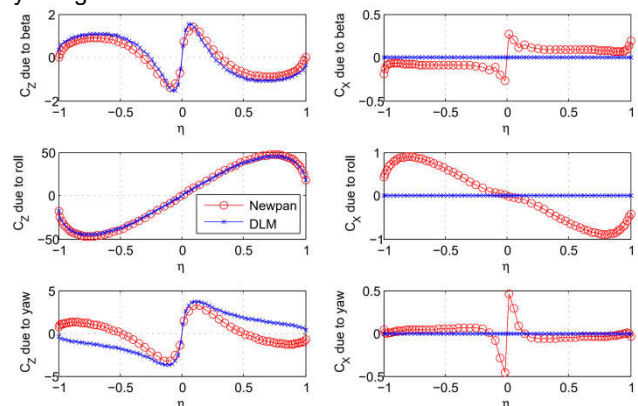

FIGURE 6 Lift and drag distribution due sideslip, roll, and yaw rate

The increased geometrical fidelity provides yet another advantage. The 3D panel method can provide surface pressures for a subsequent component loads process.

3.4 Fatigue and Damage Tolerance

During the aircraft design process, the primary structure has to be sized to withstand all loads acting on the aircraft during the entire service period. To perform this structural sizing, especially for primary fuselage structures, the PANDORA framework has been developed. For use in early design stages the framework comprises a fully parametrical Finite Element model generation and a subsequent preliminary sizing process based on strength and simplified shell stability criteria for isotropic materials [11]. The process is based on the

CPACS dataset for the description of the aircraft geometry and structural layout, such as stringer and frame distribution. Furthermore, the nodal loads acting in relevant load cases at so-called dynamic aircraft model points defined in the loads process are transferred to the FE based sizing process using the CPACS dataset.

Within the KonTeKst project the PANDORA sizing process for metallic primary fuselage structures was extended to consider aspects of fatigue and damage tolerance in addition to strength and stability criteria. In FIGURE 7 the sizing process for fatigue and damage tolerance is summarized schematically.

A first basic step (1) is the specification of requirements with respect to load cycles and inspection intervals during the full aircraft life. The Design Fatigue Goal – DFG with the total number of required loading cycles until end of service as well as the Design Service Goal – DSG with the maximum allowed load cycles between two large aircraft inspections (D-Check) are defined depending on the mission profile of the aircraft. In parallel the loads acting in the primary structure at a large number of loading conditions during a standard flight mission have to be calculated (2). The considered mission points should include all relevant segments of a flight mission, from take-off over different flight points to approach and landing with the representative weight distributions. From these data a representative load spectrum is derived for the subsequent sizing process.

A representative Finite Element model of the primary structure is generated using the PANDORA model generator based on the CPACS definition in the next step (3). The fuselage skin is modeled using shell elements while the reinforcements through stringers and frames as well as floor structures in the fuselage are modelled through beam elements. Due to the flexibility of the PANDORA framework, the internal model database can be converted to different FE solver input formats, e.g. NASTRAN, ANSYS or B2000++.

To consider fatigue and damage tolerance during the sizing process, the relevant material properties for the used materials have to be provided. These data are measured in a large number of fatigue and crack propagation tests on coupon specimens during the material qualification process. An extension of the CPACS material definition including parameters to define the Woehler Curve for fatigue as well as crack propagation curves according to definitions from Walker and Forman were proposed and implemented in the newest CPACS Schema (4) [6].

On the basis of the data defined in steps (1) to (4) the structural sizing in the PANDORA package fe_sizer is performed and a required thickness of the skin is calculated. In FIGURE 7 (5) an exemplary result of the sizing of a fuselage barrel is presented. In this plot the different contours show the relevant sizing criterion in the skin for the exemplary fuselage barrel sizing. While stability is critical in the lower fuselage with higher compression loads, Fatigue and damage tolerance are critical in the upper fuselage shell with mainly tensile loads acting from flight loads and the differential pressure during flight in high altitudes.
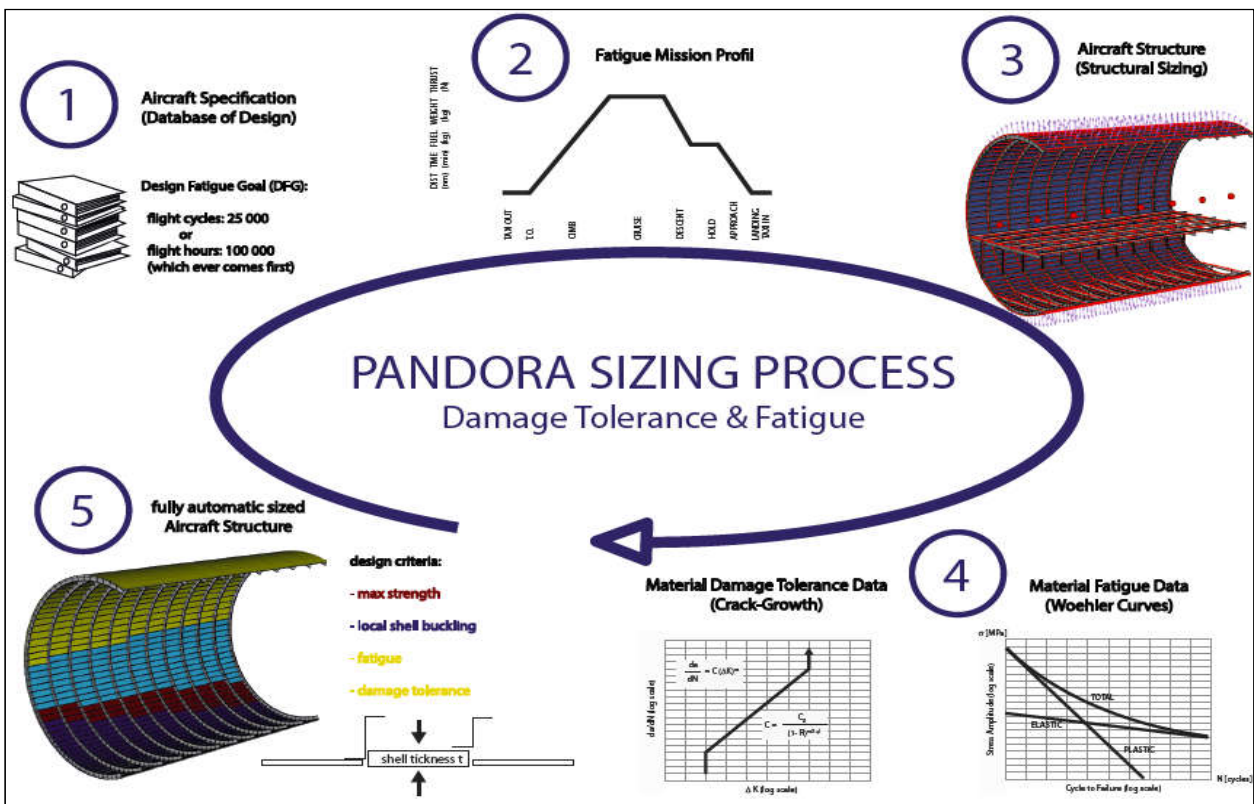

FIGURE 7 Schema for structural sizing incl. Fatigue and Damage Tolerance Criteria
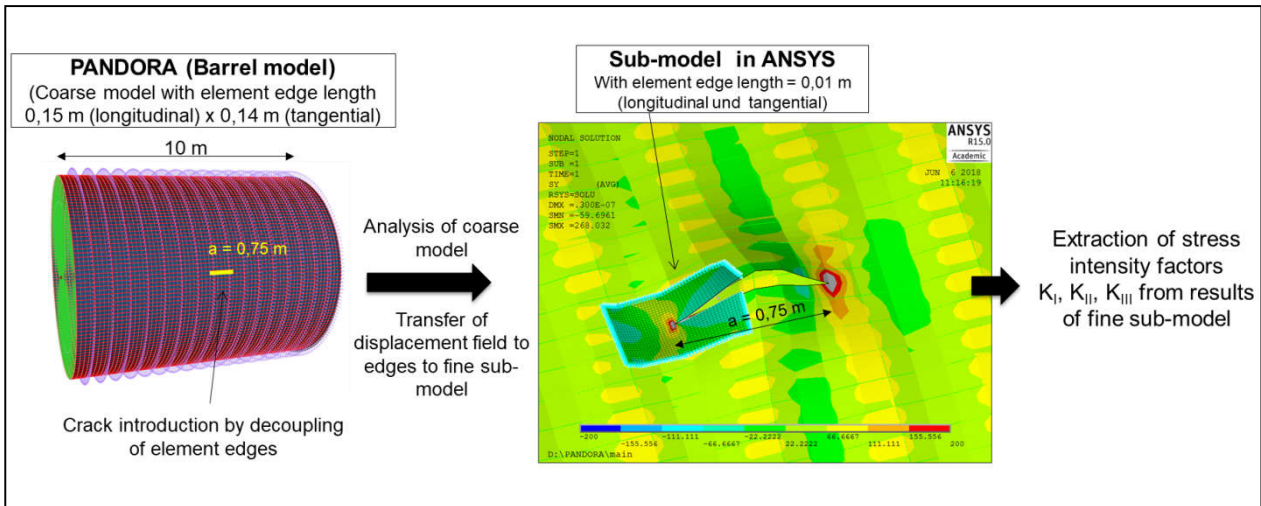
4

FIGURE 8 Coupling of models with different discretization for fracture mechanics analyses

3.5 Coupling of structural analysis with fracture mechanics analyses

A further aspect of structural analyses is the field of fracture mechanics to calculate the stresses at the crack tips and the following crack progression. To support such activities a coupling process of the global Finite Element based fuselage analysis using the PANDORA framework (§3.4) and very detailed fracture mechanics analysis was investigated. A summary of this work is shown in FIGURE 8

The process starts with the generation of a global structural model using the PANDORA framework. In this model the fuselage skin is represented by shell elements with an element edge length of more than 10 cm. This model may be generated directly from a full aircraft description in the DLR CPACS format. In a global FE model one shell element represents the skin between two adjacent stringers and frames. A local mesh refinement can then be automatically performed within the PANDORA framework close to the position, where a crack in the skin shall be analyzed. In FIGURE 8 an exemplary coarse barrel model with shell element edge length of 14-15 cm is presented. Then an initial crack is integrated into the structural model by opening the connection between adjacent shell elements. The nodes at the edges of the crack are duplicated and the corresponding element definitions updated automatically. In the example an initial crack of 75 cm length is modelled by detaching 5 shell elements from each other.

In the next step a structural analysis is performed with the coarse global model. In FIGURE 8 the equivalent stresses in the barrel are shown on the right hand side of the crack tip. Due to the loading that includes the differential pressure between the cabin and the atmosphere the crack opens and a stress concentration is generated at the crack tip.

A more detailed local model of the fuselage skin around the crack tip is than created. In this local model the geometry of the coarse model is adopted and continuum (solid) elements with a much smaller element edge length are used. In the example the edge length is reduced to 1 cm and few elements over the skin thickness allow very detailed stress analysis. The fine local model is loaded by

the displacements calculated with the coarse models using appropriate interpolation methods. In FIGURE 8 the fine local model is superposed to the initial coarse model and highlights the different discretizations. Finally stress intensity factors can be calculated from the analysis of the fine sub-model to estimate the further growth of the crack.

3.6 Potential of Aluminum Alloy for Light Weight Constructions

Materials used for aircraft fuselage structures are of strategic importance as they have a significant effect on design, production processes, maintenance costs and recycling. The idea behind their lightweight construction principle is to reduce mass and weight while ensuring predefined technical requirements. Thus, the most relevant mechanical properties for fuselage barrels are yield strength and density as shown for different material classes in FIGURE 9. A simple quotient of yield strength and density σ_f/ρ is a suitable estimation for the mass performance of an aircraft fuselage. In this case, the diagonal line refers to AA2024 as the most relevant Al alloy for aircrafts. The materials above this line have a better performance.

Because of their higher strength and lower density, composite materials are becoming increasingly important. However, since manufacturing and operating costs as well as other material properties like electrical conductivity, corrosion resistance or damage tolerance also play a role in the qualification of a material, it is always necessary to weigh up different properties [12] Therefore, advanced aluminum alloys are still crucial for structural aircraft components. In addition, improved numerical methods are able to further optimize their properties or to develop completely new alloys. Because of advantages in terms of lower density and better processability, the AlMgSc and AlLi alloys are in focus of recent investigations. In addition, high strength 7xxx with ultimate strengths > 700 MPa is increasingly used for special applications. A comparison of their specific density and Young's modulus is given in FIGURE 10.

The high temperatures needed for precipitation hardening provide advantages that other aluminum alloys do not have. Al-Mg-Sc alloys like AA5028 can be creep-formed in

the range of 325°C due to their lower yield point without a serious loss of strength. [13] This process enables cost-efficient production of double-curved fuselage shells. Compared to AA2024, AlMgSc alloys are characterized by a much higher corrosion resistance, slightly lower density (2640 kg/m³ compared to 2760 kg/m³), comparable damage tolerance properties and the possibility of fusion welding. In particular, laser beam or friction stir welding make it possible to realize integral structures without riveting. A disadvantage is the high price of the alloys resulting from the addition of Sc.
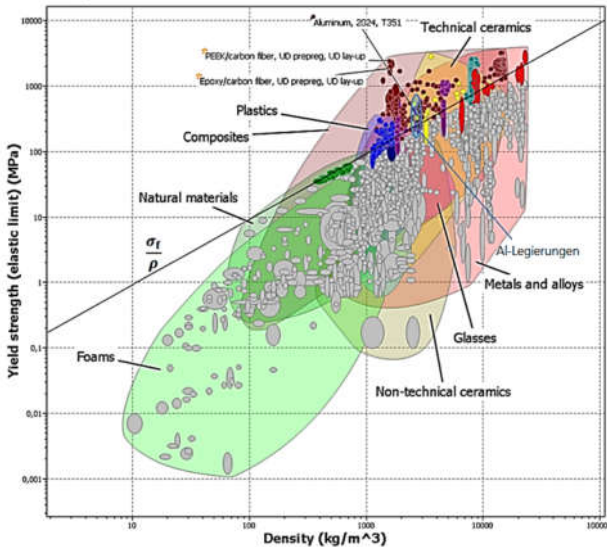

FIGURE 9 Yield strength and density for standard material classes – Source: CES Selector

Al-Li Alloys

Adding lithium to an aluminum-based alloy reduces the density by about 3 % per percent lithium content, while the Young's modulus increases by 6 %. This leads to excellent specific properties regarding Young's modulus and yield strength (see FIGURE 10). From a mechanical point of view, a serious problem is the high anisotropy of the properties (particularly in the thickness direction, that is significantly worse), which results basically from the crystallographic texture. For instance, fatigue crack paths are hard to predict based on linear-elastic fracture mechanics. Al-Li alloys are considered to be a candidate for the fuselage skin because they offer very good resistance to corrosion and stress corrosion cracking [14].

7xxx Alloys

7xxx alloys are used where high strength is required, e.g. for frames, pressure bulkheads, landing gear and as wing skin. The widely used AA7075-T6 alloy has significantly higher strengths compared to AA2024, but the disadvantage of lower fracture toughness. Unfortunately, some of the 7xxx series alloys are susceptible to stress corrosion cracking. Further optimizations of such alloys regarding less impurities can improve the strength, fracture toughness or fatigue crack growth rates.
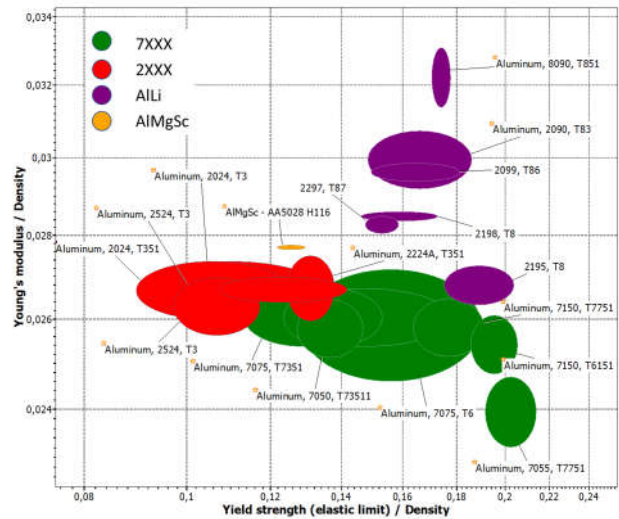

FIGURE 10 Specific Young's modulus and specific yield strength for selected lightweight aerospace alloys – Source: CES Selector

3.7 Structural Mechanics Damage Tolerance Assessment of Components out of Composite Material

Damage of composite materials

The damage tolerance (DT) assessment shall ensure the structural capability to function after a damaging event, for example a foreign object impact. The respective damage in case of a composite structure is driven by a multiplicity of potentially interacting failure modes. These multiple composite damage modes require an elaborate damage tolerance assessment in order to achieve the safety standards of a conventional metal structure. In order to exploit the lightweight potential of composite structures, advancements in the DT assessment have to be established to account for DT as early as during the preliminary design phase.

The aeronautical authorities define the possible methods to approve the DT of composites (in the Advisory Circular AC 20-107B [15]. Briefly summarized, there are three admissible concepts differing in their permissible damage growth behavior over the service life: slow growth, arrested growth and no-growth. Under compression load, an initial impact damage is likely to propagate suddenly and initiate the ultimate failure [16]. The common qualification procedures build on extensive test campaigns on the coupon level, where hardly any damage propagation occurs before the ultimate collapse under cyclic load. Very few studies analyze this topic on a larger structural scale. [17] This transfer shall be provided through the present analysis where a set of coupon tests and a campaign of sub-structural tests are combined.

DT tests on a sub-structural level

On the coupon level, the delamination encompasses a large fraction of the specimen width. Hence, the coupon offers hardly any possibility to transfer load. In a real structure with stiffening elements, a possible damage is much smaller than the load-sustaining cross section. For the present research on the DT behavior a stiffened panel is utilized, Therewith, the failure under cyclic load after impact is investigated.
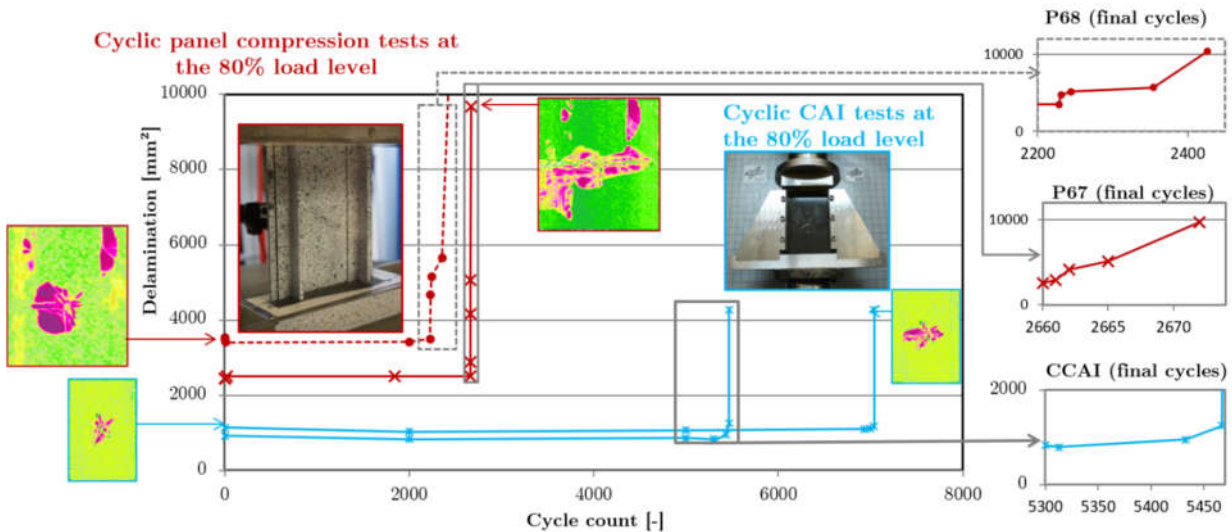
FIGURE 11 Damage propagation in the stiffened panels in comparison with the analogous coupon results

In a first step, a set of compression after impact standard coupons was subjected to cyclic load to expose the laminate-level DT behavior. In a second step, the damage propagation on a stiffened structure, the DT of this laminate was examined on a sub-structural level. For that purpose, a DT-critical panel specimen with two stiffeners was designed. The propagation of the centrical impact damage under cyclic load was monitored through in-situ ultrasonic inspection.

The results in FIGURE 11 depict the detected damage size depending on the number of load cycles with an 80% load level referring to the quasi-static residual strength of the impacted specimens. The damage propagation in the panel under force-controlled loading occurs similarly sudden as on the CAI coupons. Nonetheless, through switching to displacement control after damage growth onset, the ultimate collapse could be delayed for another 200 load cycles. In all cases, the damage did not propagate to the stiffening elements. Nonetheless, evidence for a sufficiently stable damage growth to employ a slow growth DT concept could not be found.

Structural life time until damage-growth initiation
The damage propagation interval is too short for a considerable slow growth design. Also, the damage growth is hardly detectable through standard inspection methods. However, there is a substantial period until the initiation of the damage propagation. Hence, a no-growth can be established through a modified S-N curve from the cyclic CAI coupon tests. The DT assessment in the preliminary design phase can be realized through the determination of the structural life time until the damage growth onset. The respective determination procedure can build on coupon test or on a tailored analysis method [18]. In any case, the strain allowable for a specific laminate configuration has to be calculated in order to employ a DT criterion in an early stage of the structural design

3.8 Loads Process for High Lift Wing Configuration

Loads in cruise conditions at high speeds are mostly sizing for the main structure of the aircraft. Nevertheless, loads in the low-speed regime of the aircraft at take-off, approach, and landing may become sizing in case load

alleviation technologies get matured. Additionally, they are relevant for sizing secondary structures and actuation systems.

For this reason in KonTeKst a smaller effort was taken to complete the above mentioned iLOADS loads catalogue by the relevant loads cases for low-speed conditions. Based on screening the relevant airworthiness regulations [19], 36 principal load cases for a take-off flap setting and 29 for approach/landing setting were identified, shown in FIGURE 12. These have to be accounted for at different conditions of thrust and center of gravity. Nevertheless, for those load cases several cases are identified to relate to identical aerodynamic conditions, providing some savings in the most costly analysis in terms of aerodynamics simulation.
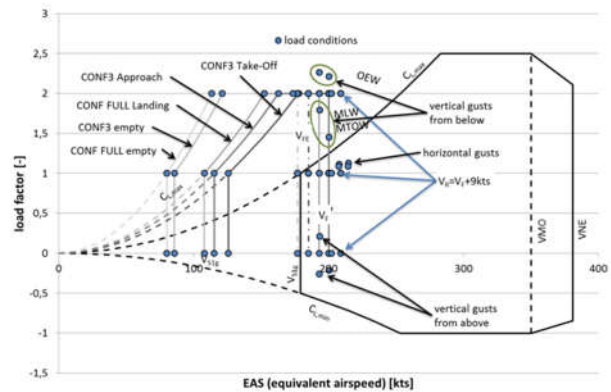

FIGURE 12 Low-speed regime load cases identified based on airworthiness regulations

In order to verify the derived loads envelope for high-lift systems, the identified loads matrix was analyzed for a set of leading edge slats of an existing aircraft. The resulting envelope of non-dimensional loads was compared to an existing aircraft's loads envelope for these parts. Exemplarily, FIGURE 13 shows a comparison for a mid-span slat device demonstrating a satisfactory capture of the relevant load conditions. These results encourage the further investigations in automatic sizing of secondary structures and actuation systems based on the DLR loads process.
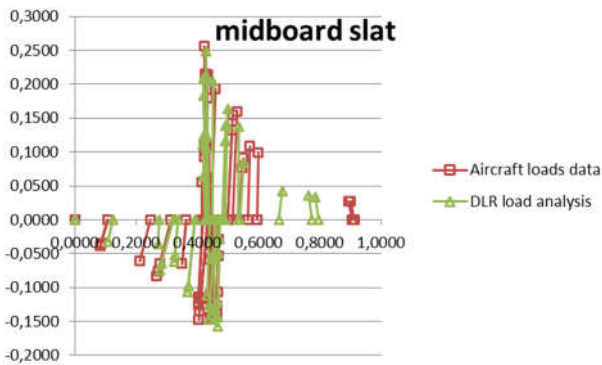
FIGURE 13 Comparison of dimensionless identified slat loads data to a loads envelope of an existing aircraft

FIGURE 14 MEMS sensor (right) compared to a one Euro coin

4. LOADS MEASUREMENT

4.1. Load Measurement at the DLR Discus-2C

For the aircraft certification process the exact determination of loads acting on the aircraft plays an important role. Forces and moments occurring during the test maneuvers are compared to design calculations and must stay within the permissible limits.

Typically conventional strain gauges (SG) are used to measure structural strains during the test maneuvers. In order to calculate the forces and moments from the measured strains an elaborate calibration process is necessary. This is usually performed on ground with the aircraft jacked up in the hangar and may last several weeks.

An alternative method is to measure the aerodynamic pressure on the component surface. This way the structural loads can be calculated by integration of the measured pressure distribution along the component surface. Compared to the SG method, the effort for calibration is significantly lower, since the pressure sensors can be calibrated without installation in the aircraft structure. The measurement of pressure distributions is usually carried out with pressure transducers and holes in the surface of the aircraft which are connected by tubes. This method requires a smooth covering of the instrumented surface and installation space for the tubes and the pressure transducers,

Sensors based on MEMS technology offer many advantageous features for this task due to their small size and the direct measurement of absolute pressures without tubes. Because of their potential benefit for flight testing, MEMS pressure sensors were already used in the certification of new aircraft designs. However, a direct comparison of load measurements based on strain gauges and based on the pressure distribution measured with MEMS sensors, can hardly be found in the literature. The two methods for load measurement in flight tests were therefore investigated in detail in the KonTeKst project

For this investigation the DLR research glider aircraft Discus-2c was used, which is equipped with several SG on the wing, fuselage and tail. Load equations for the SG system were determined during the DLR project iLOADS, which allow determining shear force, bending and torsion moment on dedicated positions of the aircraft structure.

Air data sensors and an inertial reference platform provided additional flight test data. All measurements were recorded with 100 Hz.

For the pressure measurements the MEMS pressure sensor BMP280 made by Bosch [20] and shown in FIGURE 14 was used. It is a commercial of the shelf sensor measuring absolute pressure and the local temperature. After an individual calibration of each sensor, the measurement accuracy could be increased from 1hPa to less than 20 Pa. For the load investigations 4 flexible circuit layers were designed, each one containing 16 MEMS pressure sensors. The circuit layers were embedded inside the structure of a wing glove, which could be mounted on the wing of the glider aircraft. The wing glove contained 32 MEMS pressure sensors on each side along the chord line. Holes of 0.3 mm diameter size were drilled into the wing glove to connect the sensor to the surface. The wing glove was mounted on the inner part of the RH wing near a SG load station, shown in FIGURE 15.

FIGURE 15 "Wing glove" mounted at the right wing of the Discus-2c

A flight test program with the Discus-2c glider was performed with the aim to impose different aerodynamic loads on the aircraft structure. The test maneuvers included steady conditions like trimmed wings-level flights and steady turns, as well as dynamic maneuvers like pull-up push-over and stall maneuvers. All maneuvers were performed at different velocities of 100, 130 and 160 km/h. In total 122 maneuvers from 11 flights were evaluated for the load investigation.

The base for a comparison of the two load measurement methods was the shear force measured with the SGs at the RH inner wing load station. To determine the shear force acting due to the aerodynamic load, the weight force and the inertial force were subtracted from the shear force measured by the SG. The calculation of the

shear force based on the pressure distributions measured with the MEMS sensors followed a step-by-step process. In order to compensate missing sensor information in the mid and rear parts of the airfoil, supporting points were generated for the interpolation of the pressure distribution, using the aerodynamic flow calculation program XFOIL. Two methods were investigated for the calculation of the shear force based on MEMS: One using a fitted XFOIL pressure distribution and the other using a polynomial fitting method. More details about the data processing method can be found in [21]. FIGURE 16 shows the results for a trimmed wings-level flight. The measured pressure coefficient on the wing glove surface is marked with black and white triangles for the respective upper and lower side. The measurements were averaged over the time of the steady conditions of the maneuver; error bars indicate the respective standard deviation. Integration of the pressure distribution curves leads to the shear force FZ_MEMS and FZ_XFOL in the blue box of the diagram. Both values are not far apart from the shear force measured with the SG, labeled as FZ_SG.

In total 48 steady maneuvers were evaluated with the method depicted in FIGURE 16 The shear force determined from the MEMS pressure measurements showed a qualitative good agreement with the ones determined with the SGs. Differences between the shear forces occurred, because the wing flexibility and local aerodynamic effects, could not be captured with a single wing section instrumented with the MEMS sensors. Although a simple experimental setup has been used in the investigation, the results showed that the MEMS pressure sensor technology is able to deliver load measurements of the same quality as the SGs.
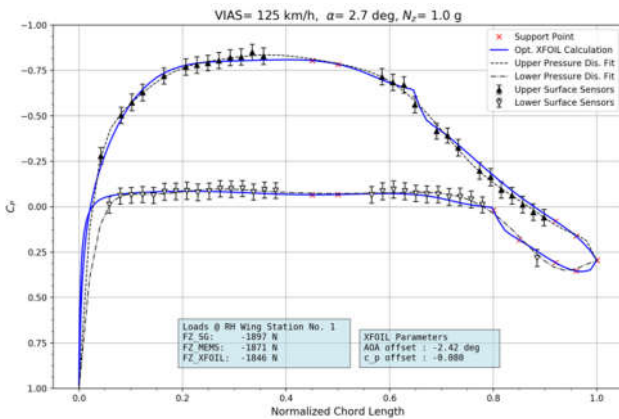

FIGURE 16 Pressure distribution

The results of the evaluation of flight maneuvers with steady loads are presented and discussed in more detail in [21]. Dynamic flight maneuvers such as pull-up push-overs and stalls haven been evaluated as well and are presented in [22]

The MEMS pressure sensor technology will be investigated under higher altitude and transonic speed conditions in the DLR project HighFly. In this case several wing and tail sections of the Falcon 2000 LX ISTAR will be instrumented with MEMS pressure sensors.

4.2. LOADS MEASURMENT AT THE DLR HALO FOR THE PMS CARRIER

Instrumentation

For an in-flight load measurement, the hanger beams – which connect the PMS carriers to the aircraft wing – are equipped with strain gauges. The suitable positions of the strain gauges are determined using FE analyses of the hanger beam.

The data acquisition during the flight is carried out using three data buses which are distributed in the aircraft. All data is channeled to a data acquisition computer, from which the data is transferred to all analysis computers in real time. A simplified block diagram is shown in FIGURE 17.
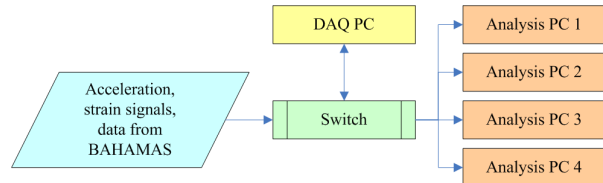

FIGURE 17 Block diagram of the data acquisition

Preparations for the flight testing

One of the tests carried out before the flight testing is the calibration of the strain gauges. In total, nine calibration load cases are applied to each PMS carrier, and the transfer matrices to estimate the loads based on the measured strains are derived. FIGURE 18 shows a load application on the PMS carrier during the calibration test. More details can be found in the references [23] and [24].
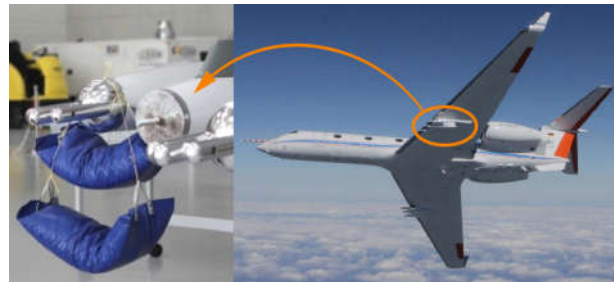

FIGURE 18 Load application for strain gauge calibration at the PMS carrier attached to the DLR HALO

Load simulations

After collecting measurement data from approx. 13 hours of flight testing, the in-house aeroservoelastic model of the HALO is adjusted according to the data to match the flight mechanical properties of the real aircraft.

The simulation results partially show a good agreement with the measured data, as can be seen in the example with the pitch moment acting on the PMS carrier during a pull up maneuver in FIGURE 19.
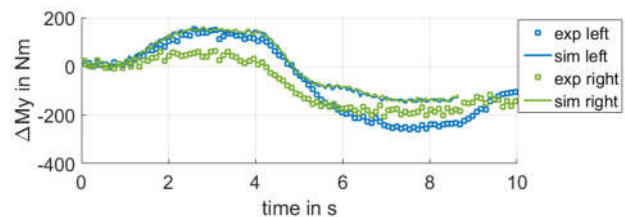

FIGURE 19 Load comparison during a pull-up maneuver between flight test and simulation

5 NUMERICAL AND EXPERIMENTAL ANALYSIS OF ACTVIVE LOAD REDUCTION

The design and testing of an active wing was a key activity to validate the design and analysis processes of the DLR Institute of Aeroelasticity in Göttingen, and the DLR Institute of System Dynamics and Control in Oberpfaffenhofen. The activities of the work package are described in detail in [25] and summarized as follows.

Firstly, a flexible composite wing of 1.6 meter (half-) span, with three flaps used for load control, was designed using the DLR aeroelastic tailoring process [26]. The Nastran wing FE model was generated with the DLR in-house parametric modeling software ModGen [27], FIGURE 20. Based on experience gathered with previous wind tunnel models, the structural layout comprised load carrying composite skins and a foam core, represented in the FE model as shell and volume elements, respectively. ModGen also provided the doublet lattice (DLM) model as well as the coupling model for the interconnection of the structural and aerodynamic model.
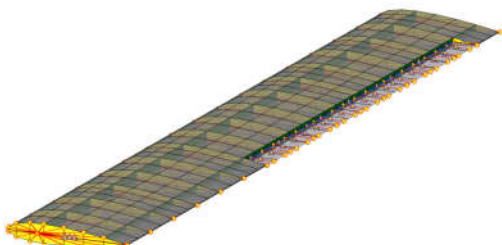

FIGURE 20 Wing finite element model

Thereby, the wing structure was optimized using different passive objective functions such as minimum wing tip deflection or maximum aileron efficiency. For each of the optimized wings, a gust load alleviation controller was designed computing suitable flap commands from distributed vertical acceleration measurements. To handle the large number of control inputs and measurements, $\mathcal{H}_2$-optimal blending techniques were used [28], where the objective was to minimize root bending moment.

Secondly, the wind tunnel model which allowed for the largest bending moment reduction was manufactured and equipped. To select suitable actuators for the control surfaces, parameters like bandwidth or positioning accuracy of different actuators were identified using a specifically designed actuator testbed [29]. Furthermore, the structural dynamic properties of the wind tunnel model were identified in a vibration test and the simulation model including the control law was updated accordingly.

Eventually, the actively controlled flexible wing was tested in the Crosswind Simulation Facility (Seitenwindkanal Göttingen, SWG) of the German Aerospace Center (DLR) in Göttingen. The closed-circuit low-speed wind tunnel operates at ambient pressure and reaches a maximum flow velocity of 65 m/s, where a main part of the experiments was conducted at 40m/s. To simulate gusts, the root of the wing was subject to pitch excitations, see FIGURE 21.The thereby induced changes in angle of attack allowed for a specific excitation of the wing.
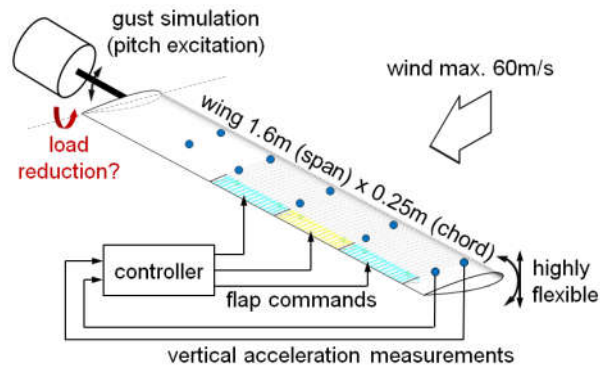

FIGURE 21 Set-up of the wind tunnel experiment

In order to validate the accuracy of the simulation model and the efficiency of the gust load alleviation controller, different gust excitations were performed and the resulting loads were measured in the wing root using a piezo balance. The gust excitations included harmonic excitations, sine-sweeps, 1-cos gusts and continuous turbulence. Additionally, different actuator fault scenarios were tested to validate the fault-tolerance of the gust load alleviation controller augmented with a fault detection and control allocation module [30]. Thereby, a load reduction of more than 50% was achieved even when simulating a jamming outer flap as depicted, e.g., in FIGURE 22.
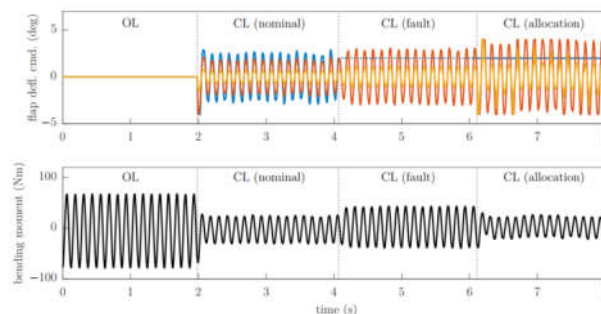

FIGURE 22 Open-loop (OL) and closed-loop (CL) results under nominal conditions (nominal) and with a jamming outer flap (fault), which is compensated using real-time control allocation (allocation).

6. CONCLUSIONS AND OUTLOOK

The presented paper layered out the comprehensive activities with respect to "aircraft loads" undertaken within the DLR project KonTeKst. They ranged from the further development of the basic assessment of DLR's loads process(es) and belonging topics via the focus on the component loads process up to experimental activities. Therewith the once with the DLR project iLOADS initiated efforts to tackle the topic aircraft loads has been continued.

Due to the prominent challenge for an even more "digitalization in aeronautics" the topic to certify an aircraft by analysis, due to massive use of computational resources, becomes more and more relevant, also regarding loads analysis. Besides the fidelity and trustworthiness of the used simulation models and the applied analysis methods, also the aspects of the provenience of the data created and processed during

extensive and partly automatically loads analysis campaigns for certification purposes is about to play an important role in the future.

Though the already existing close link between simulation models and methods and experiments, both with respect to loads analysis, there is expected to be still potential, to take advantage of the synergetic effect of linking both. That's for example evident due to new measurement technologies and manufacturing capabilities on the experimental side, but also due to a steady further development of the simulation models and methods.

With the focus only on aircraft loads the use of even more extensive and aggressive loads alleviation technologies is seen as very promising. Such direction, which is a focal point of the current DLR project oLAF (2020-2023), is expected to lead to significantly lower manoeuver and gust loads but also to influence beneficially the fatigue loads. The main goal behind such track is to reduce eventually the structural mass and to enhance the aerodynamic performance of future aircraft configurations.

CONTACT

thomas.klimmek@dlr.de

LITERATURE

[1] M. Neubauer und G. Günther, „Aircraft Loads," in *Proceedings of the RTO AVT Lecture Series on "Aging Aircraft Fleets: Structural and Other Subsystem Aspects", Sofia, Bulgaria, 13-15 November 2000*, 2000.

[2] W. R. Krüger und T. Klimmek, „Definition of a Comprehensive Loads Process in the DLR Project iLOADS," in *Deutscher Luft- und Raumfahrtkongress 2016*, 2016.

[3] W. Krüger, B. Gerlinger, O. Brodersen, T. Klimmek und Y. Günther, „Das DLR-Projekt KonTeKst: Konzepte und Technologien für emissionsarme Kurzstreckenflugzeuge," in *Deutscher Luft- und Raumfahrtkongress 2020, 1.-3. September 2020, Online*.

[4] T. Klimmek, P. Ohme, P. D. Ciampa und V. Handojo1, „Aircraft Loads - An Important Task from Pre-Design to Loads Flight Testing," in *Proceedings of Deutscher Luft- und Rumfahrtkongress 2016, 13-15 Sept. 2016, Braunschweig (Germany)*, 2016.

[5] T. Klimmek, M. Schulze, M. Abu-Zurayk, C. Ilic und A. Merle, „cpacs-MONA – An Independent and in High Fidelity Based MDO Tasks Integrated Process for the Structural and Aeroelastic Design for Aircraft Configuarations," in *IFASD2019, International Forum on Aeroelasticity and Structural Dynamics, June 10-13, 2019, Savannah (Georgia, USA)*, 2019.

[6] DLR - German Aerospace Center, „CPACS - Common Parametric Aircraft Configuration Schema," 9 2016. [Online]. Available: www.cpacs.de.

[7] N.N., *Flying Qualities of Piloted Aircraft (MIL-STD 1797A,* U. D. o. Defense, Hrsg., 1990.

[8] T. M. Kier, R. Müller und G. Looye, „Analysis of Automatic Control Function Effects on Vertical Tail Plane Critical Load Conditions," in *AIAA SciTech 2020 Forum, 6-10 January 2020, Orlando, FL, USA*.

[9] T. M. Kier, „Integrated Flexible Dynamic Maneuver Loads Models based on Aerodynamic Influence Coefficients of a 3D Panel Method," in *56th AIAA/ASCE/AHS/ASC Structures, Structural Dynamics, and Materials Conference, 5-9 January 2015, Kissimmee, FL, USA*, 2015.

[10] T. M. Kier, „An Integrated Model for Lateral Gust Loads Analysis and Dutch Roll Flight Dynamics using a 3D Panel Method," in *International Forum on Aeroelasticity and Structural Dynamics*, 2017.

[11] M. Petsch, D. Kohlgrüber und J. Heubischl, „PANDORA - A python based framework for modelling and structural sizing of transport aircraft," in *8th EASN-CEAS International Workshop*, 2018.

[12] J.-P. Immarigeon, R. T. Holt, A. K. Koul, L. Zhao, W. Wallace und J. C. Beddoes, „Lightweight materials for aircraft applications," *Materials Characterization,* Bd. 35, pp. 41-67, 1995.

[13] F. Zimmermann, A. Brosius, R.-E. Beyer, J. Standfuß, A. Jahn und D. Banke, „Creep forming of very thin AlMgSc sheets for aeronautical applications," *Procedia Manufacturing,* Bd. 15, pp. 1008-1015, 2018.

[14] R. J. Rioja und J. Liu, „The Evolution of Al-Li Base Products for Aerospace and Space Applications," *Metallurgical and Materials Transactions A,* Bd. 43, p. 3325–3337, 2012.

[15] F. A. Administration, *AC 20-107B - Composite Aircraft Structure,* 2009.

[16] A. Nettles, A. Hodge und J. Jackson, „An examination of the compressive cyclic loading aspects of damage tolerance for polymer matrix launch vehicle hardware," *Journal of Composite Materials,* p. 437–458, 2011.

[17] A. Soto, E. V. González, P. Maimí, J. A. Mayugo, P. R. Pasquali und P. P. Camanho, „A methodology to simulate low velocity impact and compression after impact in large composite stiffened panels," *Composite Structures,* Bd. 204, pp. 223-238, 2018.

[18] A. T. Rhead, R. Butler und G. W. Hunt, „Compressive strength of composite laminates with delamination-induced interaction of panel and sublaminate buckling modes," *Composite Structures,* Bd. 171, pp. 326-334, 2017.

[19] EASA, „Certification Specifications and Acceptable Means of Compliance for Large Aeroplanes," Cologne, 2016.

[20] N.N., „Datasheet BMP 280 Digital Pressure Sensor".

[21] C. Raab und K. Rohde-Brandenburger, „In-Flight Testing of MEMS Pressure Sensors for Flight Loads Determination," in *AIAA Scitech 2020 Forum*.

[22] C. Raab und K. Rohde-Brandenburger., „Dynamic Flight Load Measurements with MEMS Pressure Sensors," in *Deutscher Luft- und Raumfahrtkongress 2020, 1.-3. September 2020, Online*.

[23] V. Handojo, T. Klimmek und W. R. Krüger, „Flight Loads Analysis and Turbulence Measurements on an Atmospheric Research Aircraft," in *IFASD 2017 - International Forum on Aeroelasticity and Structural*

Dynamics, 2017.

[24] J. Sinske, Y. Govers, G. Jelicic, R. Buchbach, J. Schwochow, V. Handojo, M. Böswald und W. R. Krüger, „Flight testing using fast online aeroelastic identification techniques with DLR research aircraft HALO," in *IFASD 2017 - International Forum on Aeroelasticity and Structural Dynamics*, 2017.

[25] W. R. Krüger, J. Dillinger, M. Y. Meddaikar, J. Lübker, M. Tang, T. Meier, M. Böswald, K. I. Soal, M. Pusch und T. Kier, „Design and wind tunnel test of an actively controlled flexible wing," in *International Forum on Aeroelasticity and Structural Dynamics*, 2019.

[26] J. Dillinger, M. Y. Meddaikar, J. Lübker, M. Pusch und T. Kier, „Design and optimization of an aeroservoelastic wind tunnel model," in *IFASD 2019 - International Forum on Aeroelasticity and Structural Dynamics*, 2019.

[27] T. Klimmek, „Statische aeroelastische Anforderungen beim multidisziplinären Strukturentwurf von Transportflugzeugflügeln," 2016.

[28] M. Pusch, D. Ossmann, T. Kier, J. Dillinger, M. Tang und J. Lübker, „Aeroelastic Modeling and Control of an Experimental Flexible Wing," in *AIAA SciTech Forum*, 2019.

[29] M. Tang, M. Böswald, Y. Govers und M. Pusch, „Identification and assessment of a nonlinear dynamic actuator model for gust load alleviation in a wind tunnel experiment," in *DLRK 2019 - Deutscher Luft- und Raumfahrtkongress*, 2019.

[30] D. Ossmann und M. Pusch, „Fault Tolerant Control of an Experimental Flexible Wing," *Aerospace,* 2019.